

NJC

Accepted Manuscript



This is an *Accepted Manuscript*, which has been through the Royal Society of Chemistry peer review process and has been accepted for publication.

Accepted Manuscripts are published online shortly after acceptance, before technical editing, formatting and proof reading. Using this free service, authors can make their results available to the community, in citable form, before we publish the edited article. We will replace this *Accepted Manuscript* with the edited and formatted *Advance Article* as soon as it is available.

You can find more information about *Accepted Manuscripts* in the [Information for Authors](#).

Please note that technical editing may introduce minor changes to the text and/or graphics, which may alter content. The journal's standard [Terms & Conditions](#) and the [Ethical guidelines](#) still apply. In no event shall the Royal Society of Chemistry be held responsible for any errors or omissions in this *Accepted Manuscript* or any consequences arising from the use of any information it contains.

The structural characterization, biological activity of sulfamehtoxazolyl-azo-*p*-cresol; its copper(II) complex and their theoretical studies†

Nilima Sahu^a, Dipankar Das^a, Sudipa Mondal^a, Suman Roy^a, Paramita Dutta^a, Nayim Sepay^a, Suvroma Gupta^b, Elena López-Torres^c, and Chittaranjan Sinha^{*a}

(E)-4-((2-Hydroxy-5-methylphenyl)diazenyl)-N-(5-methylisoxazole-3-yl)benzene sulfonamide (SMX-N=N-C₆H₃(*p*-Me)-OH, **1**) and its Cu(II) complex, [Cu(SMX-N=N-C₆H₃(*p*-Me)-O)₂]_n (**2**) have been characterized by spectroscopic data and single crystal X-ray diffraction studies. The supramolecular 1D chain of **1** is constituted by inter- and intramolecular hydrogen bonds and also by π --- π interaction of aromatic rings. The complex, **2**, shows tetragonally distorted octahedral structure in which the ligand **1**, serves as N, O chelator and forms planar Cu(N,O)₂ motif; two axial positions are occupied by oxazolyl-N of neighbouring units and 3D structure is formed. The biological activities of the compounds have been evaluated against Gram positive (*B. subtilis*; IC₅₀ : 105 μ g/ml (**1**) and 105 μ g/ml (**2**)) and Gram negative bacteria (*E. coli*; IC₅₀ : 66.36 μ g/ml (**1**) and 62.2 μ g/ml (**2**)) and the complexes have better efficiency. Interactions of DNA with **1** and **2** have been examined and the binding constants are K_b(**1**), 5.920 x 10⁴ M⁻¹ and K_b(**2**), 4.445 x 10⁴ M⁻¹. The *in-silico* test is used to predict the most favoured binding mode of **1** and **2** with the active site residues of DHPS (dihydropteroate synthetase) of *E. coli* and of DNA. Cu(II) complex (**2**) binds more efficiently (CDOCKER Energy, **2**, -61.35 a.u.) in the DHPS cavity than that of ligand, **1** (CDOCKER Energy, **1**, -43.90 a.u.). The electronic structure and spectral properties of **1** and **2** have been explained by DFT and TD-DFT computation of optimized geometries of the compounds.

^aDepartment of Chemistry, Jadavpur University, Kolkata-700032, West Bengal, India;

^bDepartment of Biotechnology, Haldia Institute of Technology, Haldia, Purba Medinipur, West Bengal, Pin – 721657, India;

^cDepartamento de Química Inorgánica, c/Francisco Tomás y Valiente, 7. Universidad Autónoma de Madrid, Cantoblanco, 28049 Madrid, Spain

Correspondence: c_r_sinha@yahoo.com (C. Sinha); fax-+91-2414-6584

† CCDC 1416869 (1) and 1416868 (2). For crystallographic data in CIF or other electronic format see XXXX

1. Introduction

Sulfonamides have been the first chemotherapeutic agents effective for the treatment of bacterial infections, used as pharmaceutical products¹⁻³ and in the design of chemosensors⁴⁻⁷ and redox sensor.⁸ Sulfamethoxazole (SMX, 4-amino-*N*-(5-methylisoxazol-3-yl)-benzenesulfonamide) with trimethoprim is used as first-line therapy⁹ for prophylaxis of pneumonia caused by the fungus *Pneumocystis carinii*, a common infection in AIDS patients.¹⁰⁻¹⁴ It resists bacterial proliferation by inhibition of synthesis of dihydrofolic acid (a dihydrofolate reductase, DHFR inhibitor) *via* interference with PABA (*p*-aminobenzoic acid) in the biosynthesis of tetrahydro folic acid, which is a basic growth factor of bacteria and inhibits the activity of DHPS (Dihydropteroate synthase) protein.³ Prolong administration of SMX may cause toxicity like gastrointestinal upset, skin rashes, breathing trouble, add to the kidney damage and stomach or abdomen pain, nausea, headache.¹²⁻¹⁷ The hypersensitivity is due to oxidative metabolite like arylhydroxylamine (SMX-NHOH), nitroso aromatics (SMX-NO) in the liver.¹⁸ Development of antibiotic resistant strains and toxic metabolites are provoking to find new generation drugs by chemical modification of the traditional drugs and also synthesising metal complexes there from. Efforts have been made to synthesize different types of sulfonamides and their derivatives to have low toxic broad region antibiotics.¹⁹⁻²³ Besides, sulfonamides have been functionalised in a manner towards the design of chelating ligands for the synthesis of metal complexes those would act as more potent less toxic pharmaceutical agents.²⁴⁻³¹

Transition metal complexes have useful applications as therapeutic agents.^{32,33} Copper(II) complexes have been the subject of a large number of research studies, due to the biological role of copper(II) and its synergetic activity with the drug.³⁴ The antifungal and antibacterial properties of a range of copper(II) complexes have been evaluated against several pathogenic fungi and bacteria.³⁵⁻³⁸ Sulfonamide may coordinate to Cu(II) to generate

eight potential coordination modes and have increased the bio-ligand activity.³⁹ Recently, we have undertaken a scheme to synthesize azo (N=N)/imine (C=N) functionalized sulfonamides⁴⁰ and their 3d-transition metal complexes.⁴¹ These compounds have been used to compare anti-microbial activity with their parent sulfonamides. In this work, we report the synthesis and characterization of (E)-4-((2-hydroxy-5-methylphenyl)diazenyl)-N-(5-methylisoxazole-3-yl)benzenesulfonamide (SMX-N=N-C₆H₃(*p*-Me)-OH, **1**) and its Cu(II) complex, [Cu(SMX-N=N-C₆H₃(*p*-Me)-O)₂]_n (**2**). The structural confirmations of **1** and **2** have been carried out by single crystal X-ray diffraction data along with other physicochemical results. The electronic properties have been evaluated by DFT and TD-DFT computation using optimised structures. The molecules have been employed to examine DNA interaction by spectroscopic technique. To account the drug activity the action on Gram positive and Gram negative bacteria have been examined. The drug-protein interaction of these molecules has been computed by *in-silico* process using molecular docking studies with DHPS protein. The interaction of **1** / **2** with DNA have been examined and computed by docking studies.⁴⁰⁻⁴²

2. Experimental section

2.1. Materials and methods

Sulfamethoxazole was purchased from Hi-Media. Sodium nitrite, sodium hydroxide, *p*-cresol were available from S.D. Fine Chem. Ltd., Boisar. CuSO₄ · 5H₂O purchased from Merck, India. Solvents were purified by standard procedure.⁴³ All other chemicals were of reagent grade and were used without further purification.

Microanalytical data (C, H, and N) were collected on Perkin–Elmer 2400 CHNS/O elemental analyzer. Spectroscopic data were obtained using the following instruments: UV–Vis spectra by Perkin–Elmer UV–Vis spectrophotometer model Lambda 25; FTIR spectra (KBr disk, 4000–400 cm⁻¹) by Perkin–Elmer FT-IR spectrophotometer model RX-1; the ¹H

NMR spectra by Bruker (AC) 300/500 MHz FTNMR spectrometer. ESI mass spectra were recorded on a micro mass Q-TOF mass spectrometer (serial no. YA 263). Electrochemical measurements were performed using computer-controlled CH-Instruments, Electrochemical workstation, Model No CHI 600D (SPL) with Pt-disk electrodes. All measurements were carried out under nitrogen environment at 298 K with reference to SCE electrode in DMF using $[\text{n-Bu}_4\text{N}]\text{ClO}_4$ as supporting electrolyte. The reported potentials were uncorrected for junction potential. Magnetic susceptibility measurements of a powder crystalline sample of **2** were carried out at at Sherwood Scientific Magnetic Susceptibility Balance model Mk1 at 300 K and the data were corrected using diamagnetic corrections from Pascal's Tables.⁴⁴ The EPR spectrum was recorded at 298 K and 77 K with an X-band (9.15 GHz) Varian E-9 spectrometer. The estimation of copper in the complex (**2**) was performed by AAS (AA-400 Parkin Elemer).

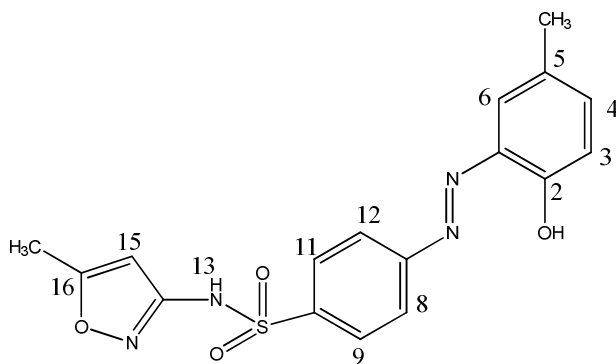
2.2. Synthesis

2.2.1. Synthesis of SMX-N=N-C₆H₃(*p*-CH₃)OH (**1**)

The sulfamethoxazolyl diazonium (SMX-N=N⁺) ion was prepared by slow addition of aqueous cold sodium nitrite (0.5 g, 7.25 mmol, 5 ml) solution to acidic solution (3N HCl, 20 ml) of sulfamethoxazole (1.0 g, 3.95 mmol) with stirring at 0-5⁰ C for 20 minutes. Intense orange yellow suspension was then added slowly to cold alkaline (2.4 gm, NaOH) solution of *p*-cresol (0.45 g, 4.16 mmol) and stirred. The pH of the reaction mixture was checked by litmus paper. An orange red precipitate appeared at pH 7 and was filtered, washed with water and dried *in-vacuo*. The product was crystallized from hot aqueous-methanol (2:1, v/v) mixture. Needle shaped bright crystals were isolated and purity was tested by TLC. Further purification was done by crystallization followed by column chromatography (silica gel, 60-120 mesh) and the desired product was eluted with chloroform-ethylacetate (9:1, v/v)

mixture. Slow evaporation of orange eluent had separated crystals; yield, 1.20 g (82%); m.p., 206(1)°C.

Microanalytical data of SMX-N=N-C₆H₃(*p*-CH₃)-OH (1) (C₁₇H₁₆N₄O₄S); Calcd : C, 54.84; H, 4.30 ; N, 15.05; Found : C, 54.72; H, 4.27 ; N, 15.00 %. Mass spectra (M+H)⁺ (m/z), 370.8. FT-IR (KBr disk; ν , cm⁻¹) : ν (C-O), 1088; ν (N=N), 1473; ν (C=N), 1620; ν (O-H), 2859; ν (S=O), 1177; ν (S-N), 682. UV-Vis spectrum (MeOH, λ /nm (10³ ϵ , cm²mol⁻¹)) 329.2 (15.24), 405.4 (6.21). ¹H NMR spectral data (DMSO-d₆): δ (5-CH₃)(*p*-cresol), 2.38 (s); δ (16-CH₃)(oxazolyl), 2.18 (s); δ (O-H), 12.40 (s); δ (N-H), 6.26 (s); δ (3-H), 6.94 (d, J = 9.0 Hz); δ (4-H), 7.20 (d, J = 9.0 Hz); δ (6-H), 7.23 (s); δ (8,12-H), 7.93 (m); δ (9,11-H), 8.00 (m); δ (15-H), 7.73 (s) ppm.



(E)-4-((2-hydroxy-5-methylphenyl)diazenyl)-N-(5-methylisoxazole-3-yl)benzenesulfonamide (HL, **1**)

2.2.2. Synthesis of [Cu(SMX-N=N-C₆H₃(*p*-CH₃)-O)₂]_n (**2**)

To aqueous solution of CuSO₄ · 5H₂O (0.08 g, 0.32 mmol) (10 ml) was added in drops methanol solution (20 ml) of SMX-N=N-C₆H₃(*p*-CH₃)-OH (1) (0.220 g, 0.59 mmol) and stirred in air for 30 mins. Then ammonia solution (1:4, v/v; 5 ml) was added and stirred for few minutes followed by refluxing for 4 h. The solution was then cooled and dark reddish

brown precipitate appeared on slow evaporation. The product was purified by slow evaporation of DMF-methanol (1:9, v/v) mixture. The crystals were deposited on glass wall and was collected and dried in a silica gel blue desiccator. Yield, 75%. Physicochemical data of copper complex : [(SMX-N=N-C₆H₃(*p*-CH₃)-O)₂Cu]_n (**2a**) Cu(C₁₇H₁₅N₄O₄S)₂, Calcd : Cu, 7.88; C, 50.64; H, 3.72; N, 13.90; Found : Cu, 7.92; C, 50.10; H, 3.68; N, 13.7 %. FT-IR (KBr disk; ν , cm⁻¹) : ν (C-O), 1095; ν (N=N), 1488; ν (C=N), 1609; ν (O-H), 2919; ν (S=O), 1142; ν (S-N), 645. UV-Vis spectrum (DMF, λ /nm ($10^3 \epsilon$, cm²mol⁻¹)) 327.5 (24.33), 400.5 (17.05), 489.3 (10.23). Magnetic moment (μ), 1.68 BM.

2.3. X-Ray crystal structure analysis

The crystals were obtained by diffusion of hexane into dichloromethane solution of **1** (0.25 x 0.20 x 0.15 mm³) while Cu(II)-complex (**2**) (0.18 x 0.17 x 0.08 mm³) was crystallized by slow evaporation of DMF-methanol mixture for a week. Data were collected by Bruker Smart CCD Area Detector at 100(2) K with θ in the range $1.37^\circ \leq \theta \leq 31.10^\circ$ for **1** and $1.81^\circ \leq \theta \leq 25.35^\circ$ for **2** respectively. Fine-focus sealed tube was used as the radiation source of graphite-monochromatized Mo-K α radiation ($\lambda = 0.71073 \text{ \AA}$). Empirical absorption correction in the $h k l$ range: $-43 \leq h \leq 41$, $-9 \leq k \leq 9$, $-25 \leq l \leq 25$ (**1**) and $-13 \leq h \leq 13$; $-16 \leq k \leq 16$; $-14 \leq l \leq 14$ (**2**) were accomplished with the program SADABS.⁴⁵ Crystallographic refinement data are collected in **Table 1**. Multi-scan absorption corrections were applied.⁴⁶ The structure was solved by direct methods with SHELXL-97⁴⁷ and refined by full-matrix least-squares techniques on F^2 using the SHELXS-97⁴⁷ program with anisotropic displacement parameters for all non-hydrogen atoms. The ORTEP-3⁴⁸ was used within WinGX⁴⁹ to prepare figures and tables for publication. Hydrogen atoms were constrained to ride on the respective carbon atoms with isotropic displacement parameters equal to 1.2 times

the equivalent isotropic displacement of their parent atom in all cases of aromatic units. Residual minimum and maximum electron densities are -0.437 and 0.484 in **1** and -0.272 and 0.310 in **2**, respectively.

2.4.1. Antimicrobial activity

The compounds, SMX-N=N-C₆H₃(*p*-CH₃)OH (**1**) and [Cu(SMX-N=N-C₆H₃(*p*-CH₃-O)₂]_n (**2**) were tested against gram e, *B. subtilis* (ATCC 6633) and gram negative, *E. coli* (ATCC 8739) bacteria. The compounds were dissolved in HPLC grade DMSO (final % of DMSO during assay was varied from 0.5-0.8% although the main stocks of the compounds were prepared using spectroscopic grade DMSO only) and stored at -20° C. All the bacterial strains were inoculated in a freshly prepared autoclaved LB broth from a 24 hours old LA slant and kept in shaker for overnight. From the overnight culture it was diluted to a final bacterial count of 1x 10⁴ cells /ml with sterile LB. The diluted culture was distributed in a number of tubes and incubated in absence as well as in presence of various concentrations of test compounds. All the tubes were incubated for 16-18 hours at 37°C in shaking condition. The OD₆₀₀ had been measured in a UV visible spectrophotometer (Shimadzu). The OD value observed in absence of test ligand had been considered as control with 100 % growth for both the bacterial species. Compared to control the relative degree of bacterial growth inhibition had been calculated for each concentration incubated under similar experimental condition from a measurement of OD at 600 nm. The minimum inhibitory concentrations (IC₅₀) *i.e.* the concentration of test compound required to inhibit the growth of bacteria by 50 % had been calculated from the % reduction of bacterial growth in comparison to control.

Table 1. Crystal data and structure refinement for **1** and **2**

	1	2
Empirical formula	C ₁₇ H ₁₆ N ₄ O ₄ S	C ₃₄ H ₃₀ N ₈ O ₈ S ₂ Cu
Formula weight	372.40	806.32
Crystal system	Monoclinic	Monoclinic
Space group	C2/c	P2(1)/c
<i>T</i> (K)	100(2)	296(2)
λ (Å)	0.71073	0.71073
<i>a</i> (Å)	29.8607(16)	11.2861(3)
<i>b</i> (Å)	6.3552(4)	13.9823(3)
<i>c</i> (Å)	17.4730(11)	11.9367(3)
β (°)	95.254(3)	91.985(2)
<i>V</i> (Å ³)	3301.9(3)	1882.55(8)
<i>Z</i>	8	2
μ (mm ⁻¹)	0.229	0.751
<i>F</i> (000)	1552	830
Density (calculated) mg/m ³	1.498	1.422
θ range for data collection /°	1.37 to 31.10	1.81 to 25.35
Independent reflections	5288	3445
Parameters	249	247
Goodness-of-fit on <i>F</i> ²	1.055	1.074
Final R indices [<i>I</i> > 2 σ (<i>I</i>)]	0.0397	
R1 ^a ,		0.0380
^b wR2	0.1012	0.0999

${}^aR = \frac{\sum |F_0 - F_c|}{\sum F_0}$. ${}^b_wR = \left[\frac{\sum w(F_0^2 - F_c^2)}{\sum w F_0^4} \right]^{1/2}$ are general but w are different, $w = 1/[\sigma^2(F_0^2) + (0.0572P)^2 + 3.4220P]$ for **1**; $w = 1/[\sigma^2(F_0^2) + (0.0719P)^2 + 0.0000P]$ for **2**.

2.4.2. Interaction of SMX-N=N-C₆H₃(*p*-CH₃)OH (**1**) and Cu(II)-complex (**2**) with calf thymus DNA. Preparation of the complex solution for DNA binding studies

Concentrated stock solution of **1** was prepared by dissolving in MeOH and **2** in DMSO and diluting suitably with tris-HCl buffer to the required concentration for the experiment. Stock solution of **2** had been prepared in DMSO because of very low solubility of **2** in MeOH and diluted using MeOH whenever necessary. All experiments were carried out using 5% DMSO solution in MeOH. Absorption spectral titration experiment was performed by keeping constant the concentration of ligand or complex with varying the CT-DNA concentration. To eliminate the absorbance of DNA itself, equal solution of CT-DNA was added both to the compound solution and to the reference one.

2.5.1. Preparation of calf thymus DNA

The tris-HCl buffer solution (pH 8.0), used in all the experiments involving CT-DNA, was prepared by using deionized and sonicated HPLC grade water (Merck). The CT-DNA used in the experiments was sufficiently free from protein. The concentration of DNA was determined with the help of its extinction coefficient, ϵ , 6600 L mol⁻¹ cm⁻¹ at 260 nm.⁵⁰ Stock solution of DNA was always stored at 4° C and used within 4 days.

2.5.2. Absorption spectroscopic studies of the complexes in presence of CT DNA

Absorption spectroscopic studies were done on a spectrophotometer (Perkin Elmer, lambda-25), using SMX-N=N-C₆H₃(*p*-CH₃)OH (**1**) (11.83 μM) with increasing

concentrations of CT DNA (from 0 μM to 13.24 μM) and in case of complex Cu(II)-complex (**2**) (45.77 μM) with increasing concentrations of CT DNA (from 0 μM to 51.82 μM). After each addition, the DNA and complex mixtures were incubated at room temperature for 15 min and scanned from 225 nm to 650 nm for the complexes. The self-absorption of DNA was eliminated in each set of experiment. Each sample was scanned for a cycle number of 2, cycle time of 5 sec at a scan speed of 100 nm/min. Modified Benesi-Hildebrand⁵¹ plot was used for the determination of ground state binding constant (K) between the complexes and CT DNA by using the relation: $A_0/\Delta A = A_0/\Delta A_{\text{max}} + (A_0/\Delta A_{\text{max}}) \times 1/K \times 1/L_t$

where $\Delta A = A_0 - A$, ΔA_{max} = maximum change in reduced absorbance, A_0 = maximum absorbance of receptor molecules (without any DNA), A = reduced absorbances of the receptor molecules (in presence of DNA), L_t = DNA concentration

2.6. Theoretical Calculations : DFT and Docking studies

The geometry optimization of **1** and **2** were carried out using density functional theory (DFT) at the B3LYP level.⁵² All calculations were carried out using the Gaussian 09 program package⁵³ with the aid of the GaussView visualization program.⁵⁴ For C, H, N, O the 6-31G (d) basis set were assigned, while for Cu and S the LanL2DZ basis set with effective core potential was employed.^{55,56} The vibrational frequency calculations were performed to ensure that the optimized geometries represent the local minima and there are only positive eigen values. Vertical electronic excitations based on B3LYP optimized geometries were computed using the time-dependent density functional theory (TD-DFT) formalism in acetonitrile using conductor-like polarizable continuum model (CPCM)⁵⁷⁻⁵⁹ Gauss Sum was used to calculate the fractional contributions of various groups to each molecular orbital.⁶⁰

The crystal structure of DHPS (Dihydroptorat Synthase of *Versinia pestis*, PDB ID 3TZF) was downloaded from RCSB protein data bank (<http://www.pdb.org>) and used for

docking. The enzyme was co-crystallized with sulfamethoxazole, 6-hydroxymethylpterin-diphosphate and magnesium ion. The *in silico* docking studies was carried out by using CDOCKER of Receptor-Ligand interactions protocol section of Discovery Studio client 3.5.⁶¹ Initially there was a pre-treatment process for both the protein and ligands. The crystal structure of **1** was used for docking. Ligand preparation was done using Prepare Ligand module in Receptor-Ligand interactions tool of Discovery studio 3.5 and prepared ligand was used for docking. Protein preparation was done under Prepare Protein module of Receptor-Ligand interactions tool of Discovery Studio 3.5 and that was used for docking. The active site was selected based on the ligand binding domain of sulfamethoxazole then the pre-existing ligand was removed and prepared ligand, **1**, was placed. Most favourable docked pose was selected according to the minimum free energy of protein-ligand complex and analysed to investigate the interaction. Absorption, distribution, metabolism, excretion and toxicity (ADMET) prediction were done in ADMET descriptor module of Small molecules protocol of Discovery studio client 3.5. Druglikeness of **1** was checked following Lipinski's rule of five.^{62,63} Using ADMET module of small molecule protocol of Discovery studio 3.5 software ADMET properties and toxicity of the compounds were checked.⁶⁴

DNA docking simulations were performed by using Hex server.⁴⁹ Crystal structures of **1** and **2** were saved in PDB format and used for docking. Crystal structure of DNA (5'-D(*CP*GP*(5HC)P*GP*AP* AP* TP*TP *CP* GP*CP*G)-3') (PDB ID 4HLI) was downloaded from the protein data bank (<http://www.rcsb.org./pdb>). Visualisation of docked pose was done in Discovery studio 3.5.

3. Results and Discussion

3.1. Synthesis and formulation of the ligand and its copper(II) complex

Low temperature (0-5°C) pH controlled diazotization of sulfamethoxazole (SMX) followed by coupling with *p*-cresol has synthesised sulfamethoxazolyl-azo-phenols (SMX-N=N-C₆H₃(*p*-CH₃)OH (**1**)). Ligand has been purified by crystallization followed by the chromatographic process prepared in silicagel column and has been eluted by chloroform-ethylacetate (9:1, v/v) mixture. The Cu(II) complex, [Cu(SMX-N=N-C₆H₃(*p*-CH₃)-O)₂]_n (**2**) has been synthesised by the reaction of methanol solution of **1** and copper sulphate in ammonical solution at refluxing condition. Reddish brown crystalline complex, **2**, has been purified by repeated crystallization in DMF-methanol mixture. Microanalytical data support composition of the complex. The complex is nonconducting in DMSO solution.

Mass spectrum of **1** supports the proposed composition and molecular ion peak (m/z) appears at 370.8 (**Supplementary Materials, Fig. S1**). Infrared spectrum of ligand shows characteristic stretching vibrations at 1473, 1620, 1177 and 682 cm⁻¹ corresponding to ν(N=N), ν(C=N), ν(S=O) and ν(S-N)⁴⁰⁻⁴² (**Supplementary Materials, Fig. S2**) and in Cu(II) complex they appear at 1483, 1616, 1142, 645 cm⁻¹ respectively and some of them have been perturbed significantly. The ¹H NMR spectrum of **1** (DMSO-d₆) shows singlet resonance at 12.44 ppm correspond to δ(OH); sulfonamide-NH (-SO₂NH-) at 6.26 ppm. Oxazolyl-CH₃ appears at 2.18 ppm while *p*-cresol -CH₃ appears at 2.38 ppm. Other aromatic protons have been characterised (6.94 – 8.00 ppm) by spin-spin interaction (**Supplementary Materials, Fig. S3**). The electronic spectrum of ligand, **1**, in methanol solution shows two high intense transition at 329.2 nm and weak band at 405 nm who are referred to π-π* and n-π* transitions.^{40,41} The complex [Cu(SMX-N=N-C₆H₃(*p*-CH₃)-O)₂]_n (**2**), in DMSO solution

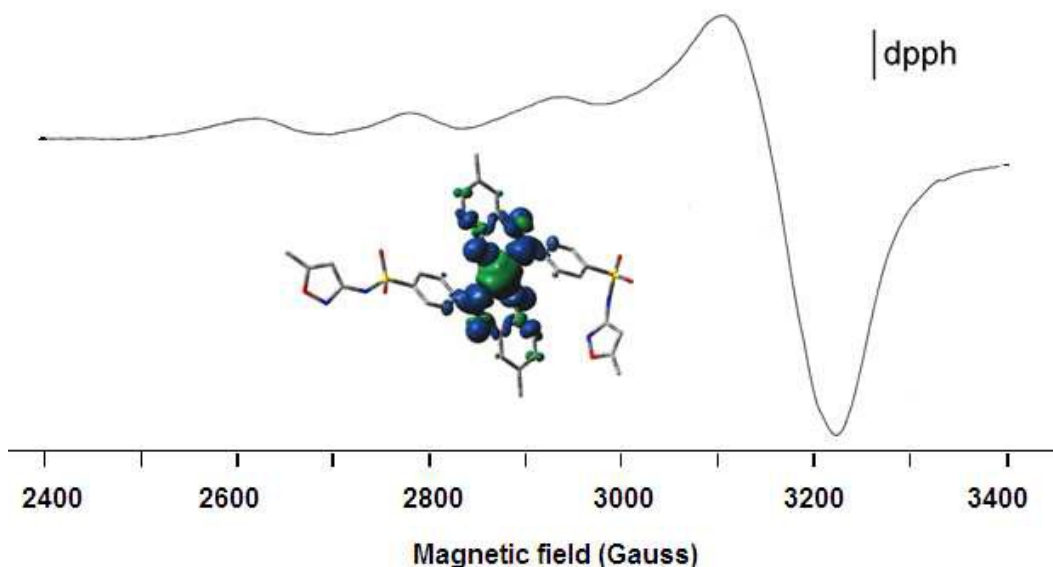


Fig.1. EPR spectrum of $[\text{Cu}(\text{SMX-N}=\text{N-C}_6\text{H}_3(p\text{-CH}_3)\text{-O})_2]_n$ in DMF solution and inset figure shows spin density distribution

shows intense band at 327.5 and 400.5 nm correspond to intra ligand transitions and very weak broad d-d band have been observed at 489 nm (**Supplementary Materials, Fig. S4**). The magnetic moment of the complex 1.68 BM at 300 K supports d^9 electronic configuration which is also supported by EPR spectrum. Polycrystalline EPR spectrum of **2** at room temperature (298 K) is weakly resolved; however, the resolution is better at 77 K. The g_{\parallel} (2.24) is greater than g_{\perp} (2.02) ($g_{\parallel} > g_{\perp} > 2.0023$) agrees with presence of unpaired electron at dx^2-y^2 of ground state configuration (**Fig. 1**).⁶⁵

3. 2. Crystal structure description of ligands and the complex

Molecular structures of SMX-N=N-C₆H₃(*p*-CH₃)OH (**1**) and $[\text{Cu}(\text{SMX-N}=\text{N-C}_6\text{H}_3(p\text{-CH}_3)\text{-O})_2]_n$ (**2**) with atom numbering scheme are shown in **Figs. 2** and **3** and selected

bond parameters are listed in **Table 2**. In **1** sulfamethoxazolyl motif is bridged by $-N=N-$ with p -Me-C₆H₃(OH)- and methyl-oxazolyl is bonded to $-SO_2NH-$ (sulfonamide) function. The

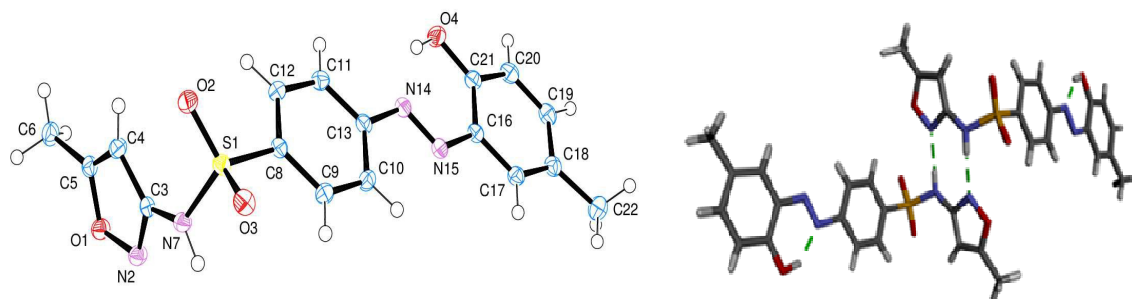


Fig. 2. Molecular structure of SMX-N=N-C₆H₃(*p*-CH₃)OH (**1**) and its hydrogen bonded dimer

S=O bond length (1.4265 (11), 1.4230 (10) Å) is corroborated with literature data. [40-42] The N(14)—N(15) bond length is 1.2654(16) Å in **1** and [Cu(SMX-N=N-C₆H₃(*p*-CH₃)-O)₂] (**2**) shows marginal elongation to N(3)—N(4), 1.272(3) Å, which is matched well with $-N=N-$ bond length reported in the literature.⁴⁰⁻⁴² The bonding strength between azo-N(15) and *p*-cresol (C(16)-N(15), 1.3975 (17) Å) is stronger than that of azo-N(14) and sulfonamide-phenyl-C(13) (C(14)-N(14), 1.4156 (17)Å). The bond angle $\angle O(2)-S(1)-O(3)$ is 121.14 (7)°. Intermolecular hydrogen bonds N(7)-(H7)-----N(2)-O(1) (N(2)---H(7), 2.03(3) Å) forms dimer and other hydrogen bonds such as C(4)—H(4)---O(2), enhances supramolecular strength. Intramolecular hydrogen bond O(4)—H(4a)---N(14) (N(14)---H(4), 1.83(3) Å; N(14)---O(4), 2.5628(17) Å) exists in the molecule (**Fig. 2b**).

The ligand serves as bidentate N, O chelating agent system [N and O refer to N(azo) and O(*p*-cresol) centers, respectively] and forms copper(II) complex, [Cu(SMX-N=N-C₆H₃(*p*-CH₃)-O)₂]_n (**2**). A distorted basal plane is constituted by Cu(N,O)₂ and two oxazolyl-N donor centres of two neighboring molecules coordinate two axial centres, 5th and 6th coordination

Table 2. Selected bond lengths and bond angles of **1** and **2**

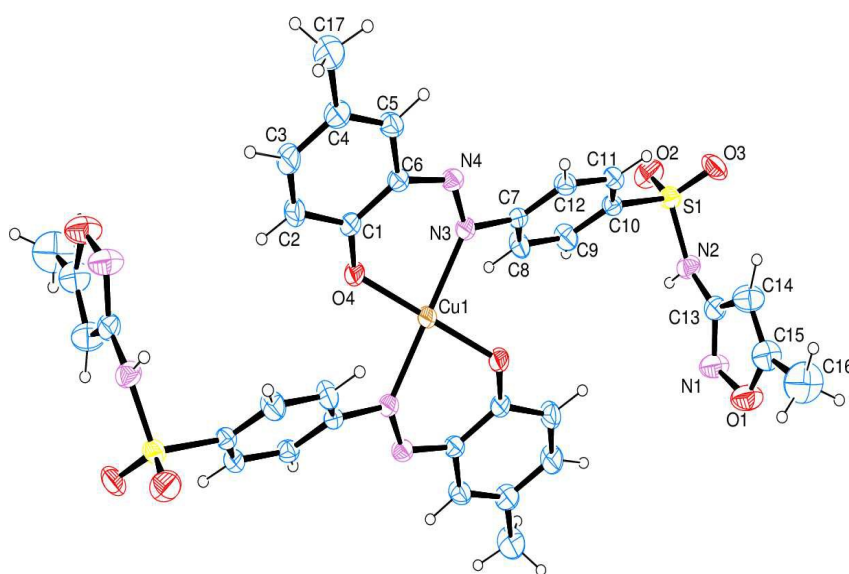
SMX-N=N-C ₆ H ₃ (<i>p</i> -CH ₃)OH (1)					
	Bond length (Å)	DFT calculated length (Å)		Bond Angle (°)	DFT calculated Angle (°)
C(3)–N(7)	1.3888(17)	1.358	O(2)–S(1)–O(3)	121.14(7)	118.9
C(13)–N(14)	1.4156(17)	1.458	N(7)–S(1)–C(8)	105.38(6)	100.5
C(16)–N(15)	1.3975(17)	1.437	S(1)–N(7)–C(3)	124.92(9)	128.3
N(14)–N(15)	1.2654(16)	1.243	C(13)–N(14)–N(15)	114.55(11)	117.4
S(1)–O(2)	1.4230(10)	1.446	C(16)–N(15)–N(14)	115.04(11)	117.9
S(1)–O(3)	1.4265(11)	1.448	N(2)–H(7)–N(7)	166.2(18)	165.4
N(7)–N(2)	2.8836(17)	2.945	N(14)–H(4)–O(4)	143.0(3)	146.7
[Cu(SMX-N=N-C ₆ H ₃ (<i>p</i> -CH ₃)-O) ₂] _n (2)					
Cu(1)–N(3) [♦]	2.017(2)	1.970	O(4)–Cu(1)–N(3)	87.64(8)	88.5
Cu(1)–O(4) [†]	1.8963(18)	1.856	O(4)–Cu(1)–N(3) [♦]	92.36(8)	90.8
Cu(1)–N(1) [#]	2.701(3)	2.884	O(4)–Cu(1)–N(1) [#]	97.34(8)	100.6
N(3)–N(4)	1.272(3)	1.316	N(3)–Cu(1)–N(1) [#]	83.49(10)	88.7
N(4)–C(6)	1.389(3)	1.350	N(3)–Cu(1)–N(1) [†]	96.52(10)	100.5
N(3)–C(7)	1.444(3)	1.426	O(1)–N(1)–Cu(1) [†]	126.87(19)	128.3
S(1)–O(2)	1.425(3)	1.388	O(4)–Cu(1)–N(3) [♦]	87.65(8)	85.7
S(1)–O(3)	1.424(3)	1.395	O(4) [♦] –Cu(1)–N(1) [#]	82.66(8)	80.9

Symmetry : [♦]2-x,1-y,2-z; [†]2-x,-1/2+y,3/2-z; [#]x,3/2-y,1/2+z

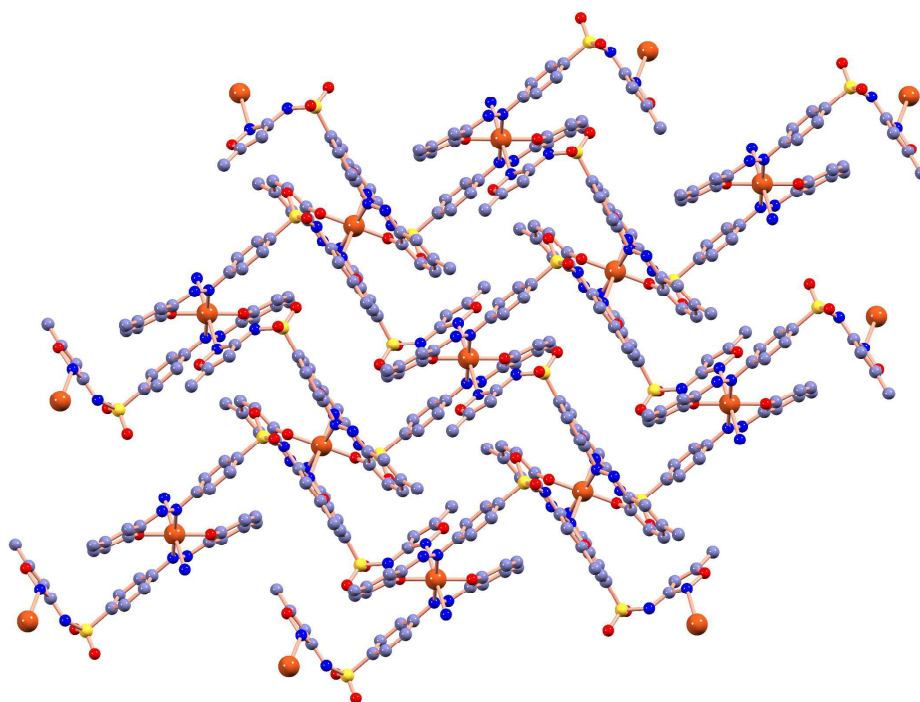
centres, to fulfill z-distorted octahedral geometry. Thus oxazolyl-N bridges and propagates to constitute a coordination polymer (**Fig. 3**). The Cu–N(azo) (Cu(1)–N(3), 2.017(2) Å) is shorter than Cu–O(phenolato) (Cu(1)–O(4), 1.8963(18) Å) bond distances. Axial Cu–N(oxazolyl) is longer (Cu(1)–N(1), 2.701 Å) than Cu–N(azo) bond data but distance is shorter than sum of van der Waals radii of copper (1.4 Å) and N(1.55, Å), and suggests weak interaction. The chelate angle $\angle O(4)–Cu(1)–N(3)$, 87.64(8)° is closer to square planar bond angle. Intermolecular H-bonds in the molecule constitute three dimensional superstructure and brings rigidity in the solid state geometry. Phenolato-O and sulfonamide-NH form a strong hydrogen bond, N(2)–H(2A)---O(4)–C(1)(phenolato) (N(2)---O(4), 2.785(4) Å; H(2A)---O(4)–(SO₂-), 2.038(2) Å; $\angle N(2)–H(2A)–O(4)$, 157(3)°; symmetry, 2-x, 1/2+y, 3/2-z). Two other H-bonds C(5)–H(5)---O(3)–(SO₂-) (C(5)---O(3), 3.386(4) Å; H(5)---O(3), 2.540(1) Å; $\angle C(5)–H(5)–O(3)$, 151.00°; symmetry, 1-x, -1/2+y, 3/2-z) and C(8)–H(8)---O(1)(oxazolyl) ((C(8)---O(1), 3.377(4) Å; H(8)---O(1), 2.460(1) Å; $\angle C(8)–H(8)–O(1)$, 168.00°; symmetry, 2-x, -1/2+y, 3/2-z) have enhanced the strength of interactions.

3.3. Antibacterial potential of the compounds and molecular docking

Sulfamethoxazole (SMX), the prominent member among sulfonamides has been a topic of interest since its first clinical use in 1935 and has been administered for the treatment and cure of infections like bacterial pneumonia, urinary tract infections, shigellosis, *Nocardia* infections and specific protozoal infections.⁶⁶ It executes antimicrobial potency by interfering with the activity of dihydropteroate synthetase that catalyzes the formation of tetrahydrofolate from *para*-amino benzoic acid (PABA). This reaction is crucial for bacterial folic acid synthesis albeit higher eukaryotes are not susceptible to SMX because of the inherent absence of folic acid synthesis pathway.



(a)

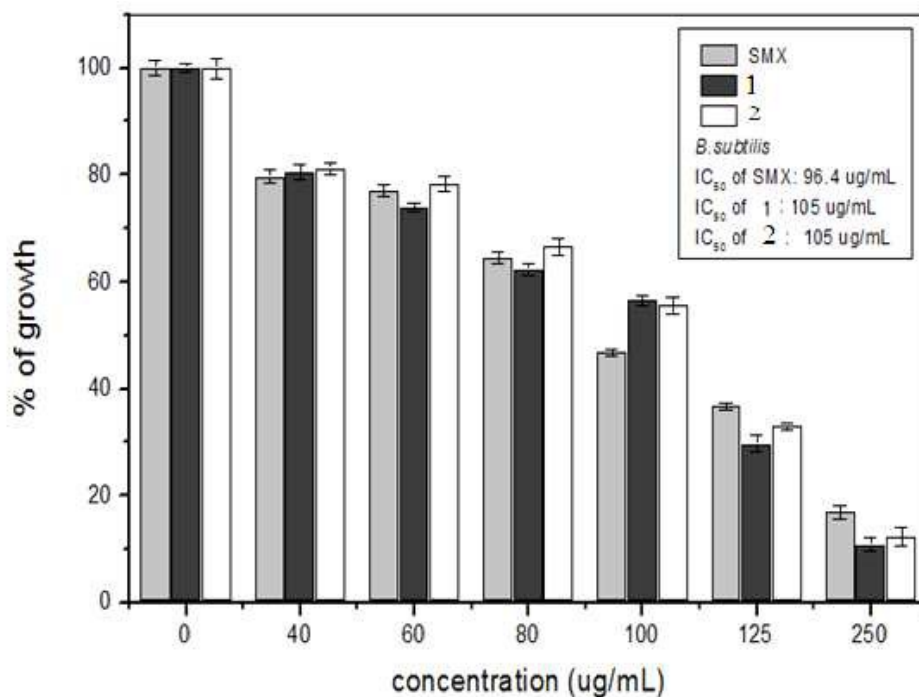


(b)

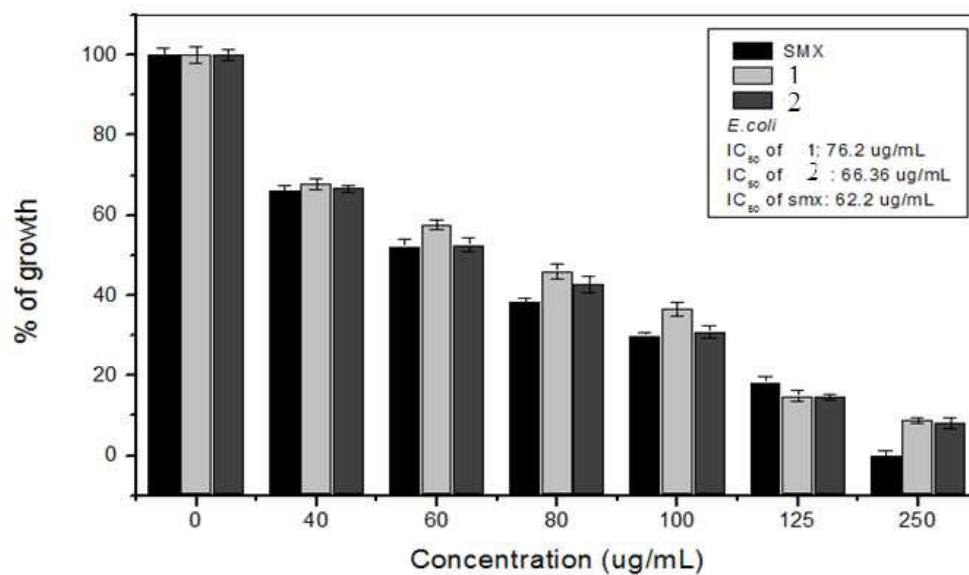
Fig. 3. (a) Molecular structure of monomer of $[\text{Cu}(\text{SMX}-\text{N}=\text{N}-\text{C}_6\text{H}_3(p\text{-CH}_3)\text{-O})_2]_n$ (**2**) (5^{th} and 6^{th} coordination positions are omitted for clarity) and (b) 3-D network

However microbes develop resistance to SMX after prolonged use due to permeability barrier/or efflux pump, mutational or recombinational changes in the target enzymes and naturally insensitive target enzymes.⁶⁷⁻⁶⁹ Additionally sulfonamides are not free from side effects like hypersensitivity and toxicity. Blood dyspraxia is also an outcome of SMX administration. But in the developing countries requirement of inexpensive drug like SMX cannot be overruled for its wide spread application due to cost effectively. That is why drive for synthesis of SMX derivatives is still in progress which may ameliorate the toxicity along with combating with the bacterial resistance against SMX. SMX-N=N-(*p*-Me)-C₆H₃OH (**1**) and its copper(II) complex (**2**) have been analysed for their bactericidal activity. The IC₅₀ *i.e.* the concentration of test compound required to inhibit the growth of bacteria by 50 % have been tested against *B. subtilis* (ATCC 6633) and *E. coli* (ATCC 8739). The profile of inhibition has been presented in **Fig. 4**. From the result it is evident that the compounds produce a concentration dependant decrease in the growth of both types of bacteria. The IC₅₀ values for **1** and **2** are 105 µg/ml for each which is 8 % less compared to SMX (96.4 µg/ml) for *B. subtilis*. On the other hand for *E. coli* the respective IC₅₀ values are 76.2 µg/ml for SMX, 66.36 µg/ml for **1** and 62.2 µg/ml for **2**. Thus, Cu(II) complexes is more efficient than its ligand, **1**. In a further study, attempt should be made to check the potency of the derivatives against resistant species of bacteria in order to validate the effectively of SMX-azo derivatives accompanied with evaluation of side effects of those newly synthesized compounds in a wide span of patient population.

Molecular docking studies has been carried out with protein structure of DHPS from *E. coli* with SMX-N=N-(*p*-Me)-C₆H₃OH (**1**) and Cu(II) complex, **2**. In contemporary research on Computational Chemistry the molecular modelling using computer aided molecular design (CAMD), lead generation and optimization, and the protein-drug interaction



(a)



(b)

Fig. 4. Inhibition profile of SMX, SMX-N=N-C₆H₃(*p*-Me)-OH (**1**) and [Cu(SMX-N=N-C₆H₃(*p*-Me)-O)₂]_n (**2**) for (a) *B. subtilis* and (b) *E. coli*

are of immense significance. Molecular docking with protein structure of the target molecule has been carried out by Discovery Studio 3.5 program.⁶¹ The best pose interaction has been concluded by docking score, binding energy and Log P data. The three dimensional (3D) structures of the ligands which were essential for docking may be obtained either from optimised structure of DFT computation or from single crystal X-ray coordinates. The drug-relevant properties of the ligands have been analyzed following Lipinski's rule of five and Dr Arup K Ghose's modified rule.^{70,71} Finally filtration was done for evaluation of druglikeness of the target molecules by ADMET (absorption, distribution, metabolism, excretion and toxicity) properties.⁷²

Different binding conformations of the molecules differing by less than 2 Å RMSD are by default grouped together in one cluster and CDOCKER interaction energy is -43.90 a.u. (1) and -61.35 a.u. (2) (Figs. 5 and 6) while sulfamethoxazole (SMX) computes the interaction energy -34.07 a.u. (Fig. 6).⁴² This implies SMX-N=N-(*p*-CH₃)-C₆H₃OH is a

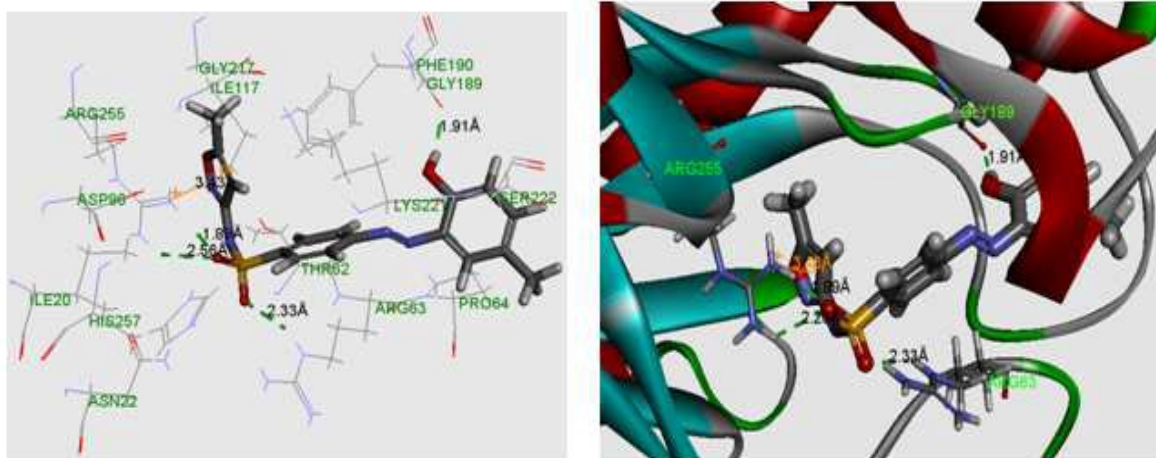


Fig. 5. Best pose binding 1AJ0@SMX-N=N-C₆H₃(*p*-Me)-OH (1) : 2D and 3D picture

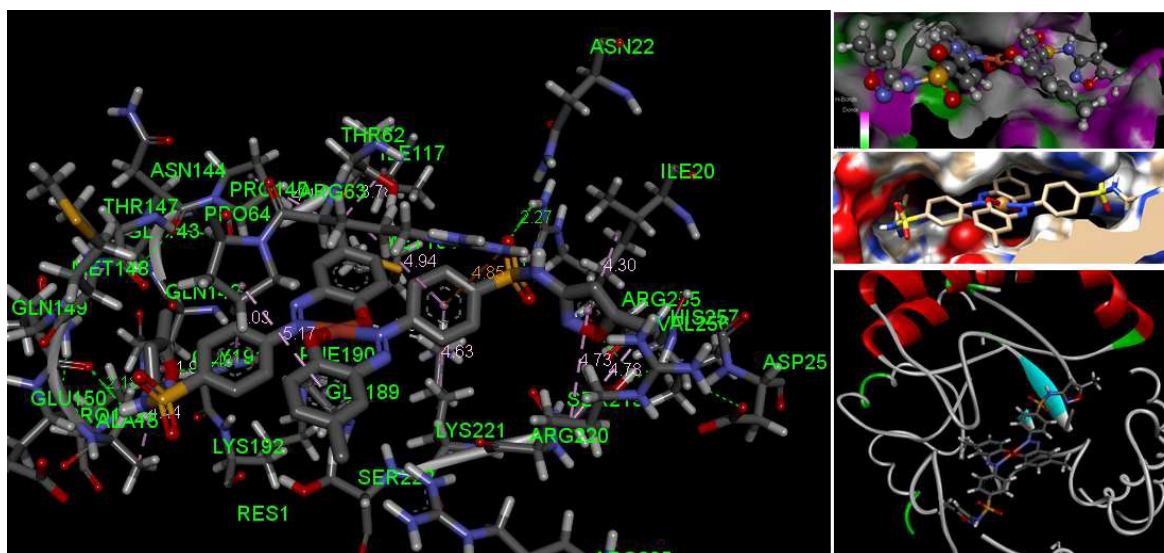


Fig. 6. Best pose binding of **2** in the DHPS cavity

strongly interacting ligand than SMX to DHPS protein. Besides, Cu(II) complex (**2**) shows best binding efficiency than that of ligand, **1**, and SMX. There are eleven amino acid residues (Asn22, Asp96, Ser222, Thr62, Arg63, Pro64, Phe190, Arg255, Lys221, His257, Ile20, Ile117, Gly217 and Gly189) interact in the binding cavity with the ligand, **1**. Interaction analysis suggests that when ligand binds with DHPS of *E. coli*, oxygen atom of $-\text{SO}_2$, oxazolyl moiety azo-N atoms form total four recognisable H-bonds with protein residue (**Figs. 5 and 6**) (Arg63N-H---O¹-(SO₂-) : N---O, 2.33 Å and $\angle\text{N-H---O}$, 146°; Arg255N-H---O¹-(SO₂-) : N---O, 1.89 and 2.56 Å and $\angle\text{N-H---O}$, 159° and 131°; Gly189-N-H---O(*p*-Me-C₆H₃-) : N---O, 1.91 Å and $\angle\text{N-H---O}$, 151°). Aromatic ring of sulfonamide is involved in π - π interaction with Arg255 (3.43 Å; **Table 3**). The docking between DHPS and [Cu(SMX-N=N-C₆H₃(*p*-Me)-O)₂]_n (**2**) shows fifteen amino acid residues in the cavity of protein (Ser219, Arg255, Glu150, Gly191, Ile20, Arg120, Arg63, Ser222, Pro64, Ala151) who bind with oxazolyl-O and O of $-\text{SO}_2\text{NH}-$ such as Ser219 N-H---O(oxazolyl) : N---O, 2.366 Å; Arg255N-H---O(SO₂), 2.042, 2.270 Å; Glu150-O---H-N(SO₂NH-), 2.180 Å; Gly191N-H---

O(oxazoly), 2.430 Å). Although many π --- π interactions are observed in the calculated structure, however, recognizable one is Pro64---phenolato ring (π --- π , 4.03 Å).

Druglikeness of ligand has been checked following Lipinski's rule of five.^{70,71} ADMET modules of discovery studio client 4.0 have been used to check ADMET (absorption, distribution, metabolism, excretion and toxicity) property of the compounds. Predicted data show that good solubility level, moderate absorption stage, six H-bond acceptors, two H-bond donors and follow Lipinski's filter and Log P is 4.07. Drug likeness and Ames prediction support non-mutagenic character of SMX-N=N-(*p*-Me)-C₆H₃OH (Supplementary Material, Tables S3, S4).

3.4. Interaction of ligand, 1 and Cu(II)-complex, 2, with CT DNA : Absorption spectroscopic studies

The interaction of transition metal complexes with DNA has received vast attention in the last two decades of research both in chemistry and biology.^{32-38, 73-75} The interaction of the metal complexes is affecting the replication and transcription of DNA and ultimately leads to the cell death.³²⁻³⁴ Over the past few years, an intensive effort has been focused to develop metal-based drugs with improved clinical effectiveness, reduced toxicity and broader spectrum of activity than that of *cisplatin*.³²⁻³⁴ Many of these complexes are very promising, and show activity on tumors which develop resistance to *cisplatin* or in which *cisplatin* is inactive.

The interactions of the complexes with chromosomal CT DNA are investigated by spectrophotometric method. When CT DNA is added with increasing concentrations to a fixed concentration of SMX-N=N-C₆H₃(*p*-Me)-OH and Cu(II)-complex the absorption is increased (Fig. 7). Such absorption characteristics may be due to the specific interaction of the ligand and complexes with DNA resulting more relax structure of the complex. At the

absorption maximum of DNA, the calculated binding constant (K) by using modified Benesi-Hildebrand plot (**Fig. 8**) for SMX-N=N-C₆H₃(*p*-Me)-OH and [Cu(SMX-N=N-C₆H₃(*p*-Me)-O)₂]_n are $5.92 \times 10^4 \text{ M}^{-1}$ and $4.445 \times 10^4 \text{ M}^{-1}$ respectively.

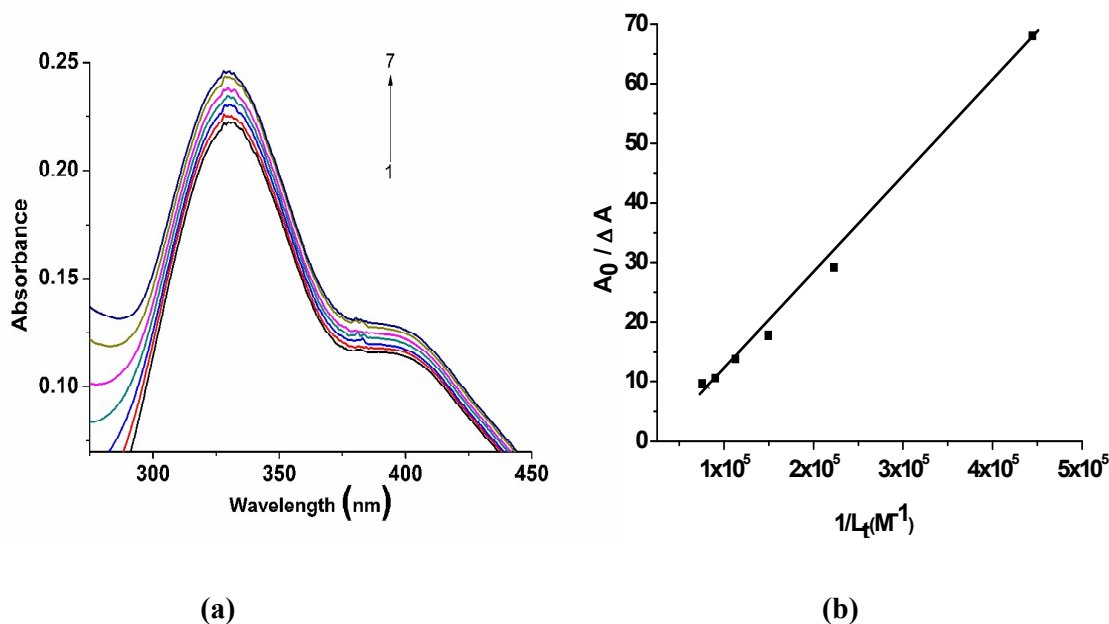


Fig. 7. (a) Absorption spectroscopic study of $11.83 \mu\text{M}$ SMX-N=N-C₆H₃(*p*-CH₃)-OH (**1**) with increasing concentrations of CT DNA (0, 2.25, 4.48, 6.70, 8.89, 11.08, 13.24 μM) respectively (1→7); (b) represents modified Benesi-Hildebrand plot for the determination of ground state binding constant between CT DNA and SMX-N=N-C₆H₃(*p*-CH₃)-OH DNA is an important target of multiple pathologies. Drugs interact with DNA in intercalation, groove binding (major and/or minor) and covalent binding. Molecular docking computation is used to explain the drug-DNA interaction.^{72,73} The docking pose of the DNA-ligand (**1**) or complex (**2**) reveals that A: C rich region is attracted.^{74,75} Azo-N of SMX-N=N-(*p*-Me)-C₆H₃OH (**1**) shows a strong hydrogen bond (DNA end A6-H---N(azo) (**1**), 2.17 Å and $\angle\text{A6-H---N}$, 145.20°) while as many as eight recognisable π --- π interactions are observed between these two participating units (**Fig. 9**; **Supplementary Materials, Table S7**).

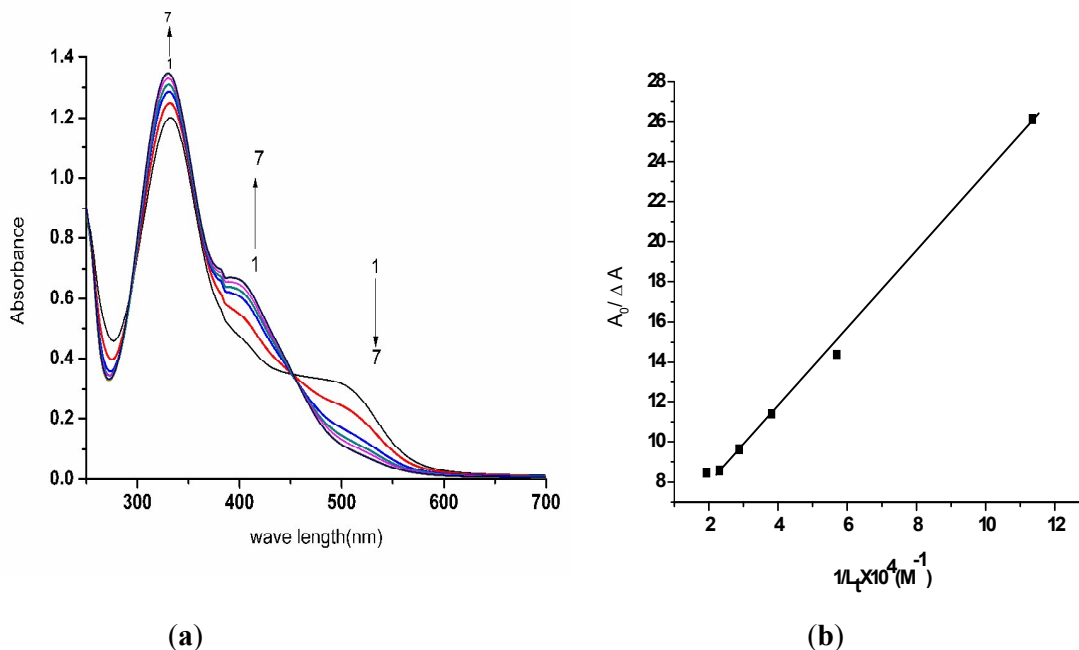


Fig. 8. (a) Absorption spectroscopic study of 45.77 μM $[\text{Cu}(\text{SMX-N}=\text{N}-\text{C}_6\text{H}_3(p\text{-Me})-\text{O})_2]_n$ (2) with increasing concentrations of CT DNA (0, 8.81, 17.55, 26.22, 34.82, 43.36, 51.82 μM) respectively (1 \rightarrow 7); (b) represents modified Benesi-Hildebrand plot for the determination of ground state binding constant between CT DNA and $[\text{Cu}(\text{SMX-N}=\text{N}-\text{C}_6\text{H}_3(p\text{-CH}_3)-\text{O})_2]_n$.

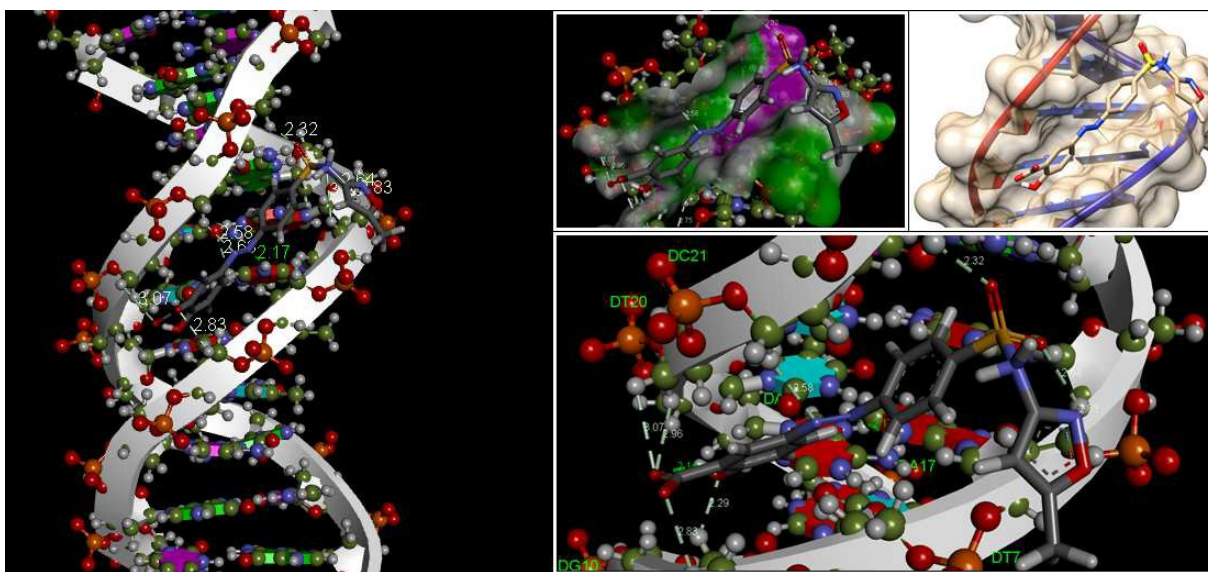


Fig. 9. DNA- SMX-N=N-(*p*-CH₃)-C₆H₃-OH (1) interaction best pose (Binding energy -6.96 a. u. ; Ligand efficiency -0.25 a.u.; Vdw H-bonded energy -9.08 a.u.)

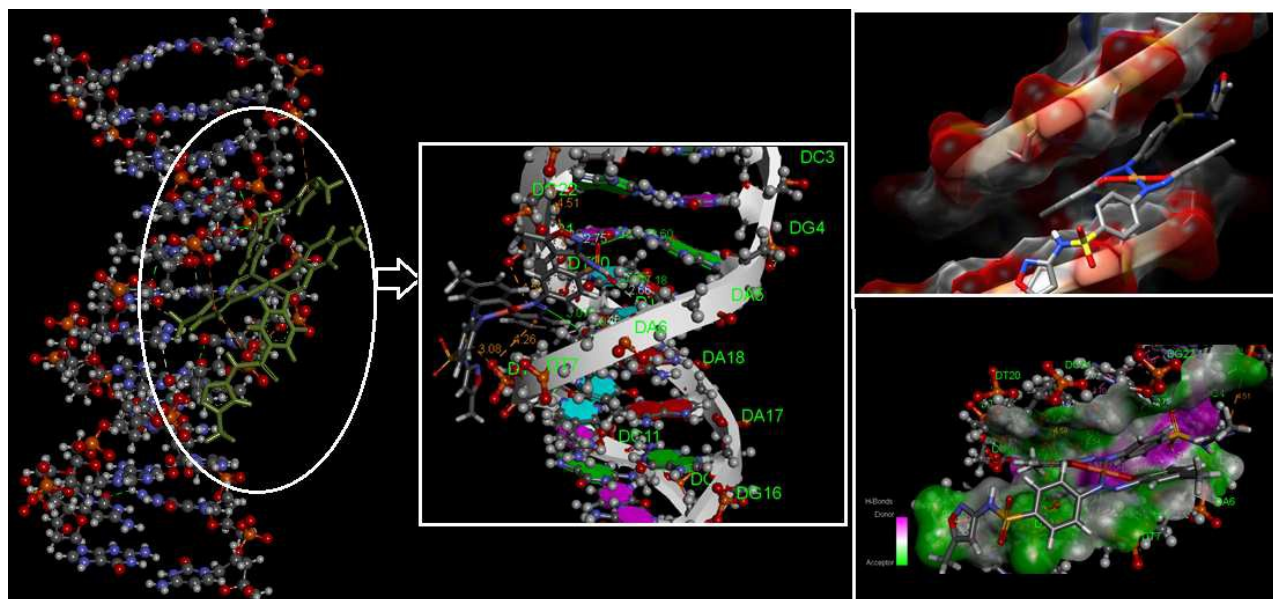


Fig. 10. DNA-[Cu(SMX-N=N-(*p*-CH₃)-C₆H₃-O)₂] (**2**) interaction best pose (Binding energy - 10.55 a.u.; Ligand efficiency -0.2 a.u.)

The DNA shows better interaction with [Cu(SMX-N=N-C₆H₃(*p*-Me)-O)₂]_n (**2**) and two recognisable H-bonds (Guanine-NH---O(SO₂NH)---: DNA end G4-NH---O(SO₂NH), 2.72 Å and ∠G4-NH---O(SO₂NH), 129.6°; Adenine A6-NH---N(azo), 3.08 Å and ∠A6-NH---N(azo), 160.01°) and six π---π interactions are computationally observed (**Fig. 10**; **Supplementary Materials, Table S8**).

3.5. The DFT Computation

The electronic structure and related properties of the ligand, **1** and the complex, **2** have been carried out using DFT computation technique; the structural agreement has also been verified on comparing the bond distances and angles between the DFT optimized and X-ray determined structures (**Table 2**). To simplify analysis of DFT computation result the structure of HL has been divided into azo, benzene sulfonamide (BSN), methyloxazolyl (MOX) and *p*-cresol

(Supplementary Material, Figs S5). The composition of MOs and proposed electronic transitions in acetonitrile (CH_3CN) solution (Supplementary Material, Tables S1 and 2) suggest that *p*-cresolato and oxazolyl rings are major electron donor while azo function and benzene sulfonamide are electron acceptors. HOMO \rightarrow LUMO (λ , 462.41 nm; f , 0.2940); HOMO-3 \rightarrow LUMO (λ , 341.15 nm; f , 0.1330); HOMO \rightarrow LUMO+2/LUMO+3 (λ , 281.74 nm; f , 0.0226) etc have been assigned as *p*-cresol to azo/benzene sulfonamide charge transferences. In the complex, $[\text{Cu}(\text{SMX-N}=\text{N}-(p\text{-Me})\text{-C}_6\text{H}_3\text{O})_2]$ (**2**) the composition of LUMO differs significantly with inclusion of 47% copper function while all other MOs remain almost similar to free ligand SMX-N=N-(*p*-Me)-C₆H₃.OH (**1**) pattern (Supplementary Material, Fig. S6, S7; Tables S3 – S6). Energy of MOs has been increased in metal complex, **2**, compared to free ligand which may be usual due to electron drifting be metal coordination (Fig. 11). The electronic spectral bands in Cu(II) complex are shifted to lower energy region along with involvement of metal orbitals for phenolato to Cu(II) transitions. The observed transitions are close to the calculated one in the molecules.

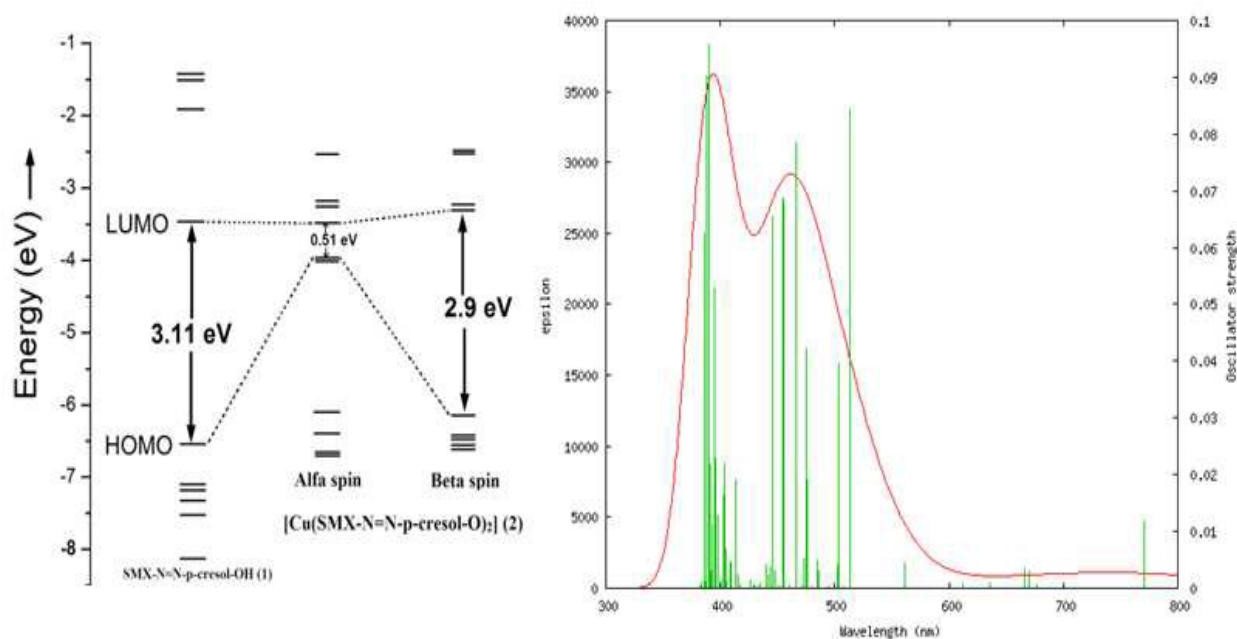


Fig.11. Correlation diagram of SMX-N=N-(*p*-CH₃)-C₆H₃OH, (**1**) and [Cu(SMX-N=N-(*p*-CH₃)-C₆H₃O)]₂ (**2**) and proposed electronic spectrum of **2**

Conclusion

Sulfamethoxazolyl-azo-*p*-cresol (SMX-N=N-(*p*-Me)-C₆H₃OH, **1**) and its copper(II) complex [Cu(SMX-N=N-(*p*-Me)-C₆H₃O)]₂ (**2**) are characterized by spectroscopic data. The ligand, **1** exists in hydrogen bonded dimer in the crystal structure while the complex, **2** is a coordination polymer which has been constituted *via* oxazolyl-N coordination to neighboring Cu(II) centre. The antibacterial activity of **1** and **2** have been performed against *B. subtilis* (ATCC 6633) and *E. coli* (ATCC 8739); Cu(II) complex (**2**) shows better efficiency than free ligand (**1**) (*B. subtilis*; IC₅₀ : 105 µg/ml (**1**) and 105 µg/ml (**2**) and *E. coli*; IC₅₀ : 66.36 µg/ml (**1**) and 62.2 µg/ml (**2**)). The *in-silico* test of the compounds with DHPS protein from *E. coli* helps to recognize the molecules in the cavity where complex prefers energetically favorable than free ligand. The DNA interaction with these two molecules also show better action with metal complex (binding constant : K_b(**1**), 5.920 x 10⁴ M⁻¹ and K_b(**2**), 4.445 x 10⁴ M⁻¹) which have been examined by docking studies. Moreover, the compound **1** is less toxic than SMX. Cu(II) complexes have versatile application in human metabolism and hence the complex **2** may be used as copper deficiency antibiotic medicine for low birth weight baby, Myelopathy (Human Swayback) and neurological disordered body etc. We are on the way to investigate these properties. The result inspires us to carry forward the pharmaceutical activity on different groups of pathogen and cells.

Supporting Information

Crystallographic data for the structure have been deposited to the Cambridge Crystallographic Data center, CCDC No. 1416869 (1) and 1416868 (2). These data can be obtained free of charge via <http://www.ccdc.cam.ac.uk/conts/retrieving.html>, or from the Cambridge Crystallographic Data Centre, 12 Union Road, Cambridge CB2 1EZ, UK; fax: (+44) 1223-336-033; or e-mail: deposit@ccdc.cam.ac.uk.

Acknowledgements

Financial support from West Bengal Department of Science and Technology (228/1(10)/(Sanc.)/ST/P/S&T/9G-16/2012), Kolkata and University Grants Commission (F.42-333/2013(SR)), New Delhi are gratefully acknowledged. We thank Dr. Tapan Kumar Mondal, Department of Chemistry, Jadavpur University for his kind help to improve quality of figure of crystal structures.

References

- 1 M. Madigan, J. Martinko, D. Stahl, D. Clark, *Brock Biology of Microorganisms* (13th ed.), Pearson Education, 2012, 797
- 2 Z. H. Chohan, H. A. Shad, *J. Enz. Inhibit. Med. Chem.*, 2012, **27**, 403-412.
- 3 H. C. Neu and T. D. Gootz., *Antimicrobial Chemotherapy, Chapter 11 in Medical Microbiology*, 4th edition (Ed. S. Baron), Galveston (TX): University of Texas Medical Branch at Galveston; (1996).
- 4 A. K. Bhoi, P. K. Sahu, G. Jha and M. Sarkar, *RSC Adv.*, 2015, **5**, 61258–61269
- 5 M. Cao, L. Jiang, F. Hu, Y. Zhang, W. C. Yang, S. H. Liu and J. Yin, *RSC Adv.*, 2015, **5**, 23666–23670
- 6 J. Huang, M. Liu, X. Ma, Q. Dong, B. Ye, W. Wang and W. Zeng, *RSC Adv.*, 2014, **4**, 22964–22970
- 7 R. Alam, T. Mistri, P. Mondal, D. Das, S. K. Mandal, A. R. Khuda-Bukhsb and M. Ali, *Dalton Trans.*, 2014, **43**, 2566–2576
- 8 H. Peng, K. Wang, C. Dai, S. Williamson and B. Wang, *Chem. Commun.*, 2014, **50**, 13668—13671
- 9 J. Zander, S. Besier, S. Faetke, S. H. Saum, V. Mueller, T. A. Wichelhaus, *Intern. J. Antimicrob. Agents*, 2010, **36**, 562-565.
- 10 C. A. Vaamonde, G. N. Contreras, J. M. Diego, *Clinical Nephrotoxins* (2nd Edition), (Ed. By B. Dee, E. Marc), 2003, 223-247.
- 11 V. Nair, M. O. Okello, A. A. Nishonov, S. K. Mishra, *PCT Int. Appl.*, 2011, WO 2011071849, A2 20110616.

- 12 G. C. Slatore, and A. S. Tilles, *Immunol. Allergy Clin. North Am.*, 2004, **24**, 477–490.
- 13 G. Choquet-Kastylevsky, T. Vial, and J. Descotes, *Curr. Allergy Asthma Rep.*, 2002, **2**, 16–25.
- 14 A. Carr, A. S. Gross, J. M. Hoskins, R. Penny, A. D. Cooper, *AIDS*, 1994, **8**, 333–337.
- 15 M. F. Gordin, L.G. Simon, B. C. Wofsy, J. Mills. *Ann. Intern. Med.*, 1984, **100**, 495–499.
- 16 L. S. Walmsley, S. Khorasheh, J. Singer, O. Djurdjev, *J Acquir Immune Defic Syndr Hum Retrovirol*, 1998, **19**, 498-505.
- 17 S. N. Lavergne, H. Wang, H. E. Callan, B. K. Park, and D. J. Naisbitt, *J Pharmacol Exp Ther.*, 2009, **331**, 372–381.
- 18 D. J. Naisbitt, J. Farrell, F. S. Gordon, L. J. Maggs, C. Burkhart, J. W. Pichler, M. Pirmohamed, K. B. Park, *Mol. Pharmaco.*, 2002, **62**, 628-637.
- 19 M. N. Arshad, M. M. Rahman, A. M. Asiri, T. R. Sobahia and S. –H. Yu, *RSC Adv.*, 2015, **5**, 81275–81281.
- 20 Y. Zhao, C. Bi, X. He, L. Chen and Y. Zhang, *RSC Adv.*, 2015, **5**, 70309–70318.
- 21 P. P. Sharp, J. –M. Garnier, D. C. S. Huang and C. J. Burns, *Med. Chem. Commun.*, 2014, **5**, 1834–1842.
- 22 W. Li, M. Beller and X. –F. Wu, *Chem. Commun.*, 2014, **50**, 9513–9516.
- 23 D. Tan, V. Štrukil, C. Mottillo and T. Frišćić, *Chem. Commun.*, 2014, **50**, 5248–5250.

- 24 S. Alyar, H. Zengin, N. Ozbek, N. Karacan, *J. Mol. Str.*, 2011, **992**, 27-32.
- 25 S. M. Tailor, U. H. Patel, *J. Mol. Str.*, 2015, **1088**, 161-168.
- 26 Z. H. Chohan, M. Z. Hernandez, F. R. Sensato, D. R. Moreira, V. R. Pereira, J. K. Neves, A. P. de Oliveira, de Oliveira, A. C., *J Enzyme Inhib. Med. Chem.*, 2014, **29**, 230-236.
- 27 M. González-Álvarez, A. Pascual-Álvarez, L. del Castillo Agudo, A. Castiñeiras, M. Liu-González, J. Borrás and G. Alzuet-Piña, *Dalton Trans.*, 2013, **42**, 10244–10259.
- 28 B. Maciás, M. V. Villa, I. García, A. Castiñeiras, J. Borra's, R. Cejudo-Marin, *Inorg. Chim. Acta*, 2003, **342**, 241 – 246.
- 29 A. M. Mansour and R. R. Mohamed, *RSC Adv.*, 2015, **5**, 5415–5423.
- 30 J. –B. Tommasino, F. N.R. Renaud , D. Luneau , G. Pilet, *Polyhedron*, 2011, **30**, 1663–1670.
- 31 B. Maciás, M. V. Villa , B. Go'mez , J. Borra's, G. Alzuet , M. Gonza'lez-A' lvarez , A. Castiñeiras, *J. Inorg. Biochem.*, 2007, **101**, 444–451.
- 32 N . Farrel, *Transition Metal Complexes as Drugs and Chemotherapeutic Agents*, Kluwer, Dordrecht, 1989.
- 33 C. Pérez a, C. V. Díaz-García, A. Agudo-López, V. Solar , S. Cabrera, M. T. Agulló-Ortuño, C. Navarro-Ranninger, J. Alemán ,, J. A. López-Martín, *Eur. J. Med. Chem.*, 2014, **76**, 360 – 368.
- 34 W. Kaim, B. Schwederski, A. Klein, *Bioinorganic Chemistry -- Inorganic Elements in the Chemistry of Life: An Introduction and Guide*, 2nd Edition, Wiley, New York, 2013.

- 35 B. Macias , I. Garcia , M. V. Villa , J. Borrás , M. Gonzalez-Alvarez , A. Castineiras, *J. Inorg. Biochem.*, 2003, **96**, 367–374.
- 36 Z. H. Chohan, H. A. Shad, M. H. Youssoufi, T. B. Hadda, *Eur. J. Med. Chem.*, 2010, **45**, 2893 – 2901.
- 37 F. Ozturk, I. Bulut, A. Bulut, *Spectrochim. Acta, Part A*, 2015, **138**, 891-899.
- 38 K. El-Baradie, R. El-Sharkawy, H. El-Ghamry, K. Sakai, *Spectrochim. Acta, A*, 2014, **121**, 180-187.
- 39 I. Beloso, J. Borrás, J. Castro, J.A. Garcia-Vazquez, P. Perez-Lourido, J. Romero, A. Sousa, *Eur. J. Inorg. Chem.*, 2004, 635–645.
- 40 D. Das, N. Sahu, S. Mondal, S. Roy, P. Dutta, S. Gupta, T. K. Mondal, C. Sinha, *Polyhedron*, 2015, **99**, 77–86
- 41 S. Mondal, S. M. Mandal, T. K. Mondal, C. Sinha, *Spectrochim. Acta A*, 2015, **150**, 268-279.
- 42 D. Das, N. Sahu, S. Roy, P. Dutta, S. Mondal, E. -L. Torres, C. Sinha, *Spectrochim Acta A*, 2015, **137**, 560-568.
- 43 A.I. Vogel , A.R. Tatchell, B.S. Furnis , A.J. Hannaford, *Vogel's Textbook of Practical Organic Chemistry* (5th Edition), Longman, 1996.
- 44 G. A. Bain, J. F. Berry, *J. Chem. Ed.*, 2008, **85**, 532-536.
- 45 Bruker, Program name. Bruker AXS Inc., Madison, Wisconsin, USA, 2001.

- 46 R. H. Blessing, *Acta Cryst. A.*, 1995, **51**, 33–38.
- 47 G. M. Sheldrick, *A short history of SHELX*, *Acta Cryst A.*, 2008, **64**, 112-122.
- 48 L.J. Farrugia, *J. Appl. Cryst.*, 1997, **30**, 565-565.
- 49 L. J. Farrugia, *J. Appl. Cryst.*, 1999, **32**, 837–838.
- 50 M. K. Paira, T. K. Mondal, D. Ojha, A. M.Z. Slawin, E. R.T. Tiekink, A. Samanta, C. Sinha, *Inorg. Chim. Acta*, 2011, **370**, 175–186.
- 51 A. M. A. Adam , M. Salman , T. Sharshar, M. S. Refat, *Int. J. Electrochem. Sci.*, 2013, **8**, 1274 – 1294.
- 52 P. J. Hay, W. R. J. Wadt, *J Chem Phys*, 1985, **82**, 299-310.
- 53 M.J. Frisch, G.W. Trucks, H.B. Schlegel, G.E. Scuseria, M.A. Robb, J.R. Cheeseman, G. Scalmani, V. Barone, B. Mennucci, G.A. Petersson, H. Nakatsuji, M. Caricato, X. Li, H.P. Hratchian, A.F. Izmaylov, J. Bloino, G. Zheng, J.L. Sonnenberg, M. Hada, M. Ehara, K. Toyota, R. Fukuda, J. Hasegawa, M. Ishida, T. Nakajima, Y. Honda, O. Kitao, H. Nakai, T. Vreven, J.A. Montgomery Jr., J.E. Peralta, F. Ogliaro, M. Bearpark, J.J. Heyd, E. Brothers, K.N. Kudin, V.N. Staroverov, R. Kobayashi, J. Normand, K. Raghavachari, A. Rendell, J.C. Burant, S.S. Iyengar, J. Tomasi, M. Cossi, N. Rega, J.M. Millam, M. Klene, J.E. Knox, J.B. Cross, V. Bakken, C. Adamo, J. Jaramillo, R. Gomperts, R.E. Stratmann, O. Yazyev, A.J. Austin, R. Cammi, C. Pomelli, J.W. Ochterski, R.L. Martin, K. Morokuma, V.G. Zakrzewski, G.A. Voth, P. Salvador, J.J. Dannenberg, S. Dapprich, A.D. Daniels, Ö. Farkas, J.B. Foresman, J.V. Ortiz, J. Cioslowski, D.J. Fox, GAUSSIAN 09, Revision D.01, *Gaussian Inc.*, Wallingford, CT, 2009.

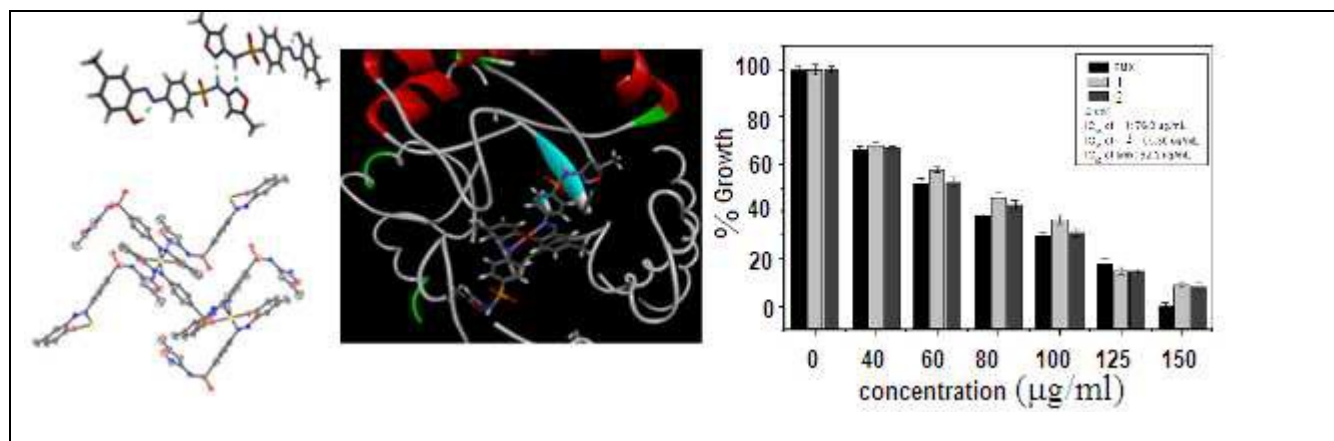
- 54 A. Frisch, A. B. Nielson, A. J. Holder, *GAUSSVIEW User Manual*, Gaussian Inc, Pittsburgh, PA, 2000.
- 55 P.J. Hay, W.R. Wadt, *J. Chem. Phys.*, 1985, **82**, 270 - 273.
- 56 W.R. Wadt, P.J. Hay, *J. Chem. Phys.*, 1985, **284**, 284 - 298.
- 57 M.E. Casida, C. Jamorski, K.C. Casida, D.R. Salahub, *J. Chem. Phys.*, 1998, **108**, 4439 - 4449.
- 58 V. Barone, M. Cossi, *J. Phys. Chem. A*, 1998, **102**, 1995 - 2001.
- 59 M. Cossi, V. Barone, *J. Chem. Phys.*, 2001, **115**, 4708 - 4717.
- 60 M.Cossi, N.Regga, G.Scalmani and V.Barone, *J.Comput.Chem.*, 2003, **24**, 669-681.
- 61 Discovery Studio 3.5 is a product of Accelrys Inc, San Diego, CA, USA.
- 62 P. Leeson, *Nature*, 2012, **481**, 455-456.
- 63 P. K. Ojha, K. Roy, *Eur. J. Med. Chem.*, 2010, **45**, 4645-4656.
- 64 S. Tabassum, M. Afzal, F. Arjmand, *Eur. J. Med. Chem.*, 2014, **74**, 694-702.
- 65 A. Datta, K.Das, C. Massera, J. K. Clegg, C. Sinha, J. -H. Huang and E. Garribba, *Dalton Trans.*, 2014, **43**, 5558-5563.
- 66 O. Sköld, *Drug Resistance Updates*, 2000, **3**, 155-160.
- 67 P. Huovinen, L. Sundström, G. Swedberg, O. Sköld, *Antimicrob Agents Chemother*, 1995, **39**, 279-289.
- 68 T. Padayachee and K. P. Klugman, *Antimicrob Agents Chemother*, 1999, **43**, 2225-2230.

- 69 G. Swedberg, S. Ringertz, O. Skoöld, *Antimicrob Agents Chemother*, 1998, 42, 1062–1067.
- 70 C. A. Lipinski, F. Lombardo, B. W. Dominy and P. J. Feeney, *Adv. Drug Deliv. Rev.*, 2001, 46, 3-26.
- 71 A. K. Ghose, V. N. Viswanadhan, J. J. Wendoloski, *J. Comb. Chem.*, 1999, 1, 55-68.
- 72 J. Shen, F. Cheng, Y. Xu, W. Li, Y. Tang, *J. Chem. Inform. Mod.*, 2010, 50, 1034-1041.
- 73 M. Roitzsch, I.B. Rother, M. Willermann, A. Erxleben, B. Costisella, B. Lippert, *Inorg. Chem.* 2002, **41**, 5946-5953.
- 74 J. Suh, *Acc. Chem. Res.* 2003, **33**, 562-570.
- 75 W.H. Ang, S. Pilet, R. Scopelliti, F. Bussy, L. Juillerat-Jeanneret, P.J. Dyson, *J. Med. Chem.* 2005, **48**, 8060-8069.

Table of Contents

The structural characterization, biological activity of sulfamehtoxazoly-azo-*p*-cresol; its copper(II) complex and their theoretical studies

Nilima Sahu, Dipankar Das, Sudipa Mondal, Suman Roy, Paramita Dutta, Nayim Sepay, Suvroma Gupta, Elena Lopez-Torrece, and Chittaranjan Sinha*



Sulfonamide-azophenol and copper(II) complexes are used for antimicrobial activity and interaction with DNA. Molecular docking has explained the mechanism of drug action.